Reliability-Based Design Sensitivity Analysis and Optimization for the Hyper-Elastic Structure Using the Meshfree Method

Young H. Park
Research Scientist
Center for Computer-Aided Design
The University of Iowa
Iowa City, Iowa 52242-1000

Nam H. Kim
Postdoctoral Associate
Center for Computer-Aided Design
The University of Iowa
Iowa City, Iowa 52242-1000

Hong J. Yim
Associate Professor
School of Mechanical and Automotive
Engineering
Kookmin University
Seoul, Korea

ABSTRACT

In this paper, efficient design sensitivity analysis (DSA) and optimization methods are presented to support reliability-based design for a hyper-elastic structure with frictional contact using a meshfree method. For the structural reliability analysis, the first-order reliability method (FORM) is utilized. The continuum-based DSA method is employed to search the most probable point (MPP) in the standard normal random variable space for structural reliability analysis. To develop the continuum-based DSA for the hyper-elastic constitutive relation and penalized contact formulation, the material derivative of continuum mechanics is utilized. The sensitivity equation is solved at each converged load step using the same tangent stiffness of response analysis due to the path dependency of the frictional contact problem. For the reliability-based structural DSA and optimization method, analytical reliability-based DSA is used to calculate the design sensitivity of reliability indices with respect to probabilistic design variables. A numerical result is presented to validate the proposed method.

NOMEMNCLATURE

$\mathbf{X}$	Random system parameter; $\mathbf{X} = [X_i]^T$ (i = 1, 2,…,n)
x	Outcomes of the random system parameter; $x = [x_i]^T$ (i = 1, 2,…,n)
x^L, x^U	Lower and upper tolerance limits of the system parameter; $x^L \leq x \leq x^U$
$\Phi(\bullet)$	Standard normal cumulative distribution function (CDF)
$G(x)$	System performance function; system fails if $G(x) < 0$
$F_G(g)$	CDF of the system performance function $G(x)$; $F_G(g) = P(G(x) < g)$
P_f	Failure probability; $P_f = F_G(0) = P(G(x) < 0)$
$\overline{P}_f$	Prescribed failure probability limit
β_G	General probability index; $\beta_G(g) = -\Phi^{-1}(F_G(g))$
β_s	Reliability index; $\beta_s = -\Phi^{-1}(F_G(0))$
g^*	Target probabilistic performance measure; $P(G(x) < g^*) = \overline{P}_f$
u^*	MPP corresponding to $G(u) = 0$ in the u-space; $\beta_s = \|u^*_{g=0}\|$
g_n	Normal gap function for contact
g_t	Tangential slip function for contact
$a_\Omega(\mathbf{z},\overline{\mathbf{z}})$	Structural variational form
$a'_V(\mathbf{z},\overline{\mathbf{z}})$	Structural fictitious load form
$a^*_\Omega(\mathbf{z};\Delta\mathbf{z},\overline{\mathbf{z}})$	Linearized structural variational form
$\ell_\Omega(\overline{\mathbf{z}})$	External load form
$\ell'_V(\overline{\mathbf{z}})$	External fictitious load form
$b_\Gamma(\mathbf{z},\overline{\mathbf{z}})$	Contact variational form
$b_N(\mathbf{z},\overline{\mathbf{z}})$	Normal contact variational form
$b_T(\mathbf{z},\overline{\mathbf{z}})$	Tangential slip variational form
$b^*_\Gamma(\mathbf{z};\Delta\mathbf{z},\overline{\mathbf{z}})$	Linearized contact variational form
$b'_V(\mathbf{z},\overline{\mathbf{z}})$	Contact fictitious load form

INTRODUCTION

In engineering design, the traditional deterministic design optimization model (Arora, 1989; Haftka and Gurdal, 1991) has been successfully applied to systematically reduce the cost and improve quality. However, the existence of uncertainties in either engineering simulations or manufacturing processes requires a

reliability-based design optimization (RBDO) model for robust and cost-effective designs. In the RBDO model for robust system parameter design, the mean values of random system parameters are chosen as design variables, and the cost function is minimized subject to prescribed probabilistic constraints. The probabilistic constraint can be directly prescribed by the reliability index evaluated in the traditional first-order reliability analysis (Enevoldsen, 1994; Enevoldsen and Sorensen, 1994; Chandu and Grandi, 1995; Frangopol and Corotis, 1996; ; Wu and Wang, 1996; Yu et al., 1997; Grandhi and Wang, 1998). The probabilistic constraint can also be evaluated using the performance measure approach (Tu et al., 1999).

The first-order reliability method (FORM) which introduces the first-order approximation at the most probable point (MPP) to obtain structural reliability is practically very efficient. However, for FORM, the first-order sensitivities of the structural performance with respect to random variables are required. Therefore, an accurate and efficient approach for sensitivity analysis of failure functions is highly desirable for the general application of FORM for structural problems.

In this paper, the frictional contact problem for hyper-elastic structural systems using the meshfree method is considered for RBDO. For nonlinear analysis of the hyper-elastic material, an effective numerical method, which can handle material incompressibility under large deformation, is highly desirable for the analysis of rubber components. The meshfree method is an ideal choice since, unlike the conventional FEA method, it is not affected by the mesh distortion problem. To accelerate computations for FORM and RBDO, a continuum-based DSA method was employed to perform an accurate and efficient sensitivity analysis of the failure function. A continuum-based shape design sensitivity formulation for a hyper-elastic structure with frictional contact has been developed using the material derivative of continuum mechanics and penalized contact formulation (Kim et al., 2000) and is utilized in this paper. For numerical analysis of the frictional contact problem, the reproducing kernel particle method (RKPM) (Liu et al., 1995; Chen et al., 1998) is utilized, and, thus, sensitivity calculation. To handle material incompressibility under large deformation, a pressure projection method (Chen et al., 1996) which is a generalization of the B-bar method (Hughes, 1987) for linear problems to avoid volumetric locking for nearly incompressible materials is used.

GENERAL DEFINITION OF THE RBDO MODEL

For the random system parameter $\mathbf{X} = [X_i]^T$ (i = 1, 2,…, n), the system performance criteria are described by the system performance functions $G(\boldsymbol{x})$ such that the system fails if $G(\boldsymbol{x}) < 0$. The statistic description of $G(\boldsymbol{x})$ is characterized by its cumulative distribution function (CDF) $F_G(g)$ as

$$F_G(g) = P(G(\boldsymbol{x}) < g) = \int_{G(\boldsymbol{x})<g} \ldots \int f_{\mathbf{X}}(\boldsymbol{x})dx_1\ldots dx_n,$$
$$\boldsymbol{x}^L \leq \boldsymbol{x} \leq \boldsymbol{x}^U \tag{1}$$

where $f_{\mathbf{X}}(\boldsymbol{x})$ is the joint probability density function (JPDF) of all random system parameters and g is named the probabilistic performance measure. The probability analysis of the system performance function is to evaluate the non-decreasing $F_G(g)\sim g$ relationship (Tu et al., 1999), which is performed in the probability integration domain bounded by the system parameter tolerance limits given in Eq. (1).

A generalized probability index β_G, which is a non-increasing function of g, is introduced (Madsen et al., 1986) as

$$F_G(g) = \Phi(-\beta_G) \tag{2}$$

which can be expressed in two ways using the following inverse transformations (Rubinstein, 1981; Tu et al., 1999), respectively, as

$$\beta_G(g) = -\Phi^{-1}(F_G(g)) \tag{3a}$$
$$g(\beta_G) = F_G^{-1}(\Phi(-\beta_G)) \tag{3b}$$

Thus, the non-increasing $\beta_G\sim g$ relationship represents a one-to-one mapping of $F_G(g)\sim g$ and also completely describes the probability distribution of the performance function.

In the robust system parameter design, the RBDO model (Enevoldsen and Sorensen, 1994; Chandu and Grandi, 1995; Wu and Wang, 1996; Yu et al., 1997; Grandhi and Wang, 1998) can generally be defined as

$$\begin{aligned} &\text{minimize} \quad \text{Cost}(\mathbf{d}) &(4a)\\ &\text{subject to} \quad P_{f,j}=P(G_j(\boldsymbol{x}) < 0) \leq \overline{P}_{f,j}, \ j = 1, 2,\ldots, np &(4b)\\ &\qquad\qquad \mathbf{d}^L \leq \mathbf{d} \leq \mathbf{d}^U &(4c) \end{aligned}$$

where the cost can be any function of the design variable $\mathbf{d} = [d_i]^T \equiv [\mu_i]^T$ (i = 1, 2, …, n), and each prescribed failure probability limit $\overline{P}_f$ is often represented by the reliability target index as $\beta_t = -\Phi^{-1}(\overline{P}_f)$. Hence, any probabilistic constraint in Eq. (4b) can be rewritten using Eq. (1) as

$$F_G(0) \leq \Phi(-\beta_t) \tag{5}$$

which can also be expressed in two ways through inverse transformations as

$$\beta_s = -\Phi^{-1}(F_G(0)) \geq \beta_t \tag{6a}$$
$$g^* = F_G^{-1}(\Phi(-\beta_t)) \geq 0 \tag{6b}$$

where β_s is traditionally called the reliability index and g^* is named the target probabilistic performance measure.

To date, most researchers have used the reliability index approach (RIA) of Eq. (6a). In this paper, RIA is used to directly prescribe the probabilistic constraint as

$$\beta_s(\mathbf{d}) \geq \beta_t \tag{7a}$$

At a given design $\mathbf{d}^k = [d_i^k]^T \equiv [\mu_i^k]^T$, the evaluation of reliability index $\beta_s(\mathbf{d}^k)$ for RIA is performed using the well-developed reliability analysis (Madsen et al., 1986) as

$$\beta_s(\mathbf{d}^k) = -\Phi^{-1}(\int_{G(\boldsymbol{x})<0} \ldots \int f_{\mathbf{X}}(\boldsymbol{x})dx_1\ldots dx_n),$$
$$\boldsymbol{x}^L \leq \boldsymbol{x} \leq \boldsymbol{x}^U \tag{7b}$$

FORM FOR APPROXIMATE PROBABILITY INTEGRATION

The evaluation of Eq. (7a) requires reliability analysis where the multiple integration is involved as shown in Eq. (7b), and the exact probability integration is in general extremely complicated to compute. The Monte Carlo simulation (MCS) (Rubinstein, 1981) provides a convenient approximation for reliability because it

directly approximates the $\beta_G \sim g$ relationship. However, MCS becomes prohibitively expensive for many engineering applications.

Some approximate probability integration methods have been developed to provide efficient solutions (Breitung, 1984; Madsen et al., 1986; Tvedt, 1990), such as FORM or the asymptotic SORM. The FORM often provides adequate accuracy and is widely accepted for RBDO applications. The RIA can be used effectively with FORM or SORM in the probabilistic constraint evaluation. This paper focuses on RBDO using FORM for approximate probability integration.

General Interpretation of FORM

In FORM, the transformation (Hohenbichler and Rackwitz, 1981; Madsen et al., 1986) from the nonnormal random system parameter $\mathbf{X}$ (x-space) to the independent and standard normal variable $\mathbf{U}$ (u-space) is required. If all system parameters are mutually independent, the transformations can be simplified as

$$u_i = \Phi^{-1}(F_{X_i}(x_i)), \quad i = 1, 2, \ldots, n \qquad (8a)$$

$$x_i = F_{X_i}^{-1}(\Phi(u_i)), \quad i = 1, 2, \ldots, n \qquad (8b)$$

The performance function $G(\mathbf{x})$ can then be represented as $G_U(\mathbf{u})$ in the u-space. The point on the hypersurface $G_U(\mathbf{u}) = 0$ with the maximum joint probability density is the point with the minimum distance from the origin and is named the most probable point (MPP) $\mathbf{u}_{g=0}^*$. The minimum distance, named the first-order reliability index $\beta_{s,FORM}$, is an approximation of the generalized probability index corresponding to g_a as

$$\beta_{s,FORM} \approx \beta_s = \beta_G(0) \qquad (9)$$

Thus, the first-order reliability analysis is to find the MPP on the hypersurface $G_U(\mathbf{u}) = 0$ in the u-space, and MPP $\mathbf{u}_{g=0}^*$ is found by performing first-order reliability analysis in RIA.

First-Order Reliability Analysis

In traditional first-order reliability analysis (Madsen et al., 1986), the first-order reliability index $\beta_{s,FORM}$ is the solution of a nonlinear optimization problem

$$\begin{array}{ll} \text{minimize} & \|\mathbf{u}\| \qquad (10a) \\ \text{subject to} & G_U(\mathbf{u}) = 0 \qquad (10b) \end{array}$$

where the optimum is the MPP $\mathbf{u}_{g=0}^*$ and thus $\beta_{s,FORM} = \|\mathbf{u}_{g=0}^*\|$. Many MPP search algorithms (such as HL-RF, Modified HL-RF, AMVFO) and general optimization algorithms (such as SLP, SQP, MFD, augmented Lagrangian method, etc.) can be used to find the MPP (Wu and Wirsching, 1987; Wu et al., 1990; Wang and Grandhi, 1994).

DESIGN SENSITIVITY ANALYSIS OF MULTIBODY FRICTIONAL CONTACT PROBLEM

Response Analysis of Contact Problem

For the multibody contact problem, the contact point depends on the motion of a slave body and a master body together since the second body also moves as it deforms. The normal contact condition prevents penetration of one body into another and the tangential slip represents frictional behavior of the contact surface. A regularized Coulomb friction law proposed by Wriggers et al. (1990) is utilized in this paper.

Contact Condition

Figure 1 shows a general contact condition between two bodies in R^2. Body 1 is referred to as the slave body and body 2 as the master body. The surface coordinate of the master body $\mathbf{x}_c \in \Gamma_c^2$ can be represented by a natural coordinate ξ along the master surface. As the point $\mathbf{x} \in \Gamma_c^1$ on the slave surface is in contact with the point $\mathbf{x}_c \in \Gamma_c^2$ on the master surface, $\mathbf{x}_c$ can be represented using the natural coordinate ξ_c at the contact point as $\mathbf{x}_c(\xi_c)$. The contact point moves as the slave body is deformed by the change of ξ_c in addition to the deformation of the master body. The tangential vector at $\mathbf{x}_c(\xi_c)$ along the master surface can be obtained by $\mathbf{t}(\xi_c) = \mathbf{x}_{c,\xi}$ where comma represents the partial derivative.

The normal contact condition can be imposed on the structure by measuring the distance between parts of the boundaries Γ_c^1 and Γ_c^2. The impenetration condition can be defined, using the normal gap function g_n which measures the normal distance, as

$$g_n \equiv (\mathbf{x} - \mathbf{x}_c(\xi_c))^T \mathbf{e}_n(\xi_c) \geq 0, \qquad \mathbf{x} \in \Gamma_c^1, \ \mathbf{x}_c \in \Gamma_c^2 \qquad (11)$$

where $\mathbf{e}_n(\xi_c) = \mathbf{e}_3 \times \mathbf{e}_t$ is the unit outward normal vector of the master surface at the contact point, $\mathbf{e}_t = \mathbf{t} / \|\mathbf{t}\|$ is the unit tangential vector, and $\mathbf{e}_3$ is the unit vector out of plane direction fixed in R^2. The contact point $\mathbf{x}_c \in \Gamma_c^2$ corresponding to the slave surface point $\mathbf{x} \in \Gamma_c^1$ is determined by solving the following contact consistency condition

$$\varphi(\xi_c) = (\mathbf{x} - \mathbf{x}_c(\xi_c))^T \mathbf{e}_t(\xi_c) = 0 \qquad (12)$$

Note that, in Eq. (12), $\mathbf{x}_c(\xi_c)$ is the closest projection point of $\mathbf{x} \in \Gamma_c^1$ onto the master surface. As the contact point moves along the master surface, a frictional force that resists the tangential relative movement exists along the tangential direction of the surface of the master body. The tangential slip function g_t is the measure of the relative movement of the contact point along the master surface as

$$g_t \equiv \|\mathbf{t}^0\|(\xi_c - \xi_c^0) \qquad (13)$$

where $\mathbf{t}^0$ and ξ_c^0 are the tangential vector and natural coordinate of the previous converged time step, respectively.

If there exists a region Γ_c which violates the impenetration conditions of Eq. (11), it is penalized by the penalty function. Similarly, the tangential movement of Eq. (13) can also be penalized. Define the contact penalty function for the violated region by

$$P = \frac{1}{2}\omega_n \int_{\Gamma_c} g_n^2 \, d\Gamma + \frac{1}{2}\omega_t \int_{\Gamma_c} g_t^2 \, d\Gamma \qquad (14)$$

where ω_n and ω_t are the penalty parameters for normal contact and tangential slip, respectively. The contact variational form can be obtained by taking the first-order variation of P as

$$b(\mathbf{z}, \bar{\mathbf{z}}) \equiv \overline{P} = \omega_n \int_{\Gamma_c} g_n \bar{g}_n \, d\Gamma + \omega_t \int_{\Gamma_c} g_t \bar{g}_t \, d\Gamma \qquad (15)$$

where $\omega_n g_n$ and $\omega_t g_t$ correspond to the compressive normal force and tangential traction force, respectively.

For the variational equation, the contact variational form in Eq. (15) needs to be expressed in terms of the displacement variation. For the convenience of the derivations to follow, define several scalar symbols

$$\alpha \equiv \mathbf{e}_n{}^T \mathbf{x}_{c,\xi\xi}, \beta \equiv \mathbf{e}_t{}^T \mathbf{x}_{c,\xi\xi}, \gamma \equiv \mathbf{e}_n{}^T \mathbf{x}_{c,\xi\xi\xi}, c \equiv \|\mathbf{t}\|^2 - g_n \alpha,$$
$$\nu \equiv \|\mathbf{t}\| \|\mathbf{t}^0\| / c \tag{16}$$

The variations of the normal gap and tangential slip functions can be obtained by considering the variation of the contact consistency condition in Eq. (12) as

$$\overline{g}_n(\mathbf{z};\overline{\mathbf{z}}) = (\overline{\mathbf{z}} - \overline{\mathbf{z}}_c)^T \mathbf{e}_n = \hat{\overline{\mathbf{z}}}^T \mathbf{e}_n \tag{17a}$$

$$\overline{g}_t = \|\mathbf{t}^0\| \overline{\xi}_c = \nu \hat{\overline{\mathbf{z}}}^T \mathbf{e}_t + (g_n \|\mathbf{t}^0\| / c) \overline{\mathbf{z}}_{c,\xi}{}^T \mathbf{e}_n \tag{17b}$$

where $\hat{\mathbf{z}} = \mathbf{z} - \mathbf{z}_c$ is the relative displacement between the slave and master contact points.

Using Eqs. (17a) and (17b), the contact variational form of Eq. (15) can be rewritten in terms of the variation of the displacement as

$$b(\mathbf{z},\overline{\mathbf{z}}) = b_N(\mathbf{z},\overline{\mathbf{z}}) + b_T(\mathbf{z},\overline{\mathbf{z}}) \tag{18a}$$

where

$$b_N(\mathbf{z},\overline{\mathbf{z}}) = \omega_n \int_{\Gamma_c} g_n \hat{\overline{\mathbf{z}}}^T \mathbf{e}_n \, d\Gamma \tag{18b}$$

$$b_T(\mathbf{z},\overline{\mathbf{z}}) = \omega_t \int_{\Gamma_c} g_t \left(\nu \hat{\overline{\mathbf{z}}}^T \mathbf{e}_t + (g_n \|\mathbf{t}^0\| / c) \overline{\mathbf{z}}_{c,\xi}{}^T \mathbf{e}_n \right) d\Gamma \tag{18c}$$

are the normal contact and tangential slip variational form, respectively. Note that the frictional effect in Eq. (18a) also acts in the normal direction by the displacement variation of the master surface

Figure 2 shows a friction curve used in this paper. The stick condition occurs when the frictional traction force generated by the tangential slip and the penalty parameter is less than the normal force multiplied by the frictional coefficient

$$|\omega_t g_t| \leq |\mu \omega_n g_n| \tag{19}$$

Otherwise, it becomes a slip condition. In Eq. (19), μ is the Coulomb friction coefficient. For the case of the slip condition, the tangential slip variational form of Eq. (18c) is written as

$$b_T(\mathbf{z},\overline{\mathbf{z}}) = -\mu \omega_n \operatorname{sgn}(g_t) \int_{\Gamma_c} g_n \left(\nu \hat{\overline{\mathbf{z}}}^T \mathbf{e}_t + (g_n \|\mathbf{t}^0\| / c) \overline{\mathbf{z}}_{c,\xi}{}^T \mathbf{e}_n \right) d\Gamma \tag{20}$$

Variational Principle for Finite Deformation with Frictional Contact Problem

The Mooney-Rivlin type material model with nearly incompressible constraint is used in this paper. The nearly incompressibility constraint can be formulated using a perturbed Lagrangian formulation (Chang et al., 1991) or a penalty method on conjunction with a pressure projection (Chen et al., 1996) as a generalization of the perturbed Lagrangian formulation.

For the case of hyper-elastic material with a frictional contact problem, the variational principle for virtual work can be written as

$$a(\mathbf{z},\overline{\mathbf{z}}) + b(\mathbf{z},\overline{\mathbf{z}}) = \ell(\overline{\mathbf{z}}), \quad \forall \overline{\mathbf{z}} \in Z \tag{21}$$

where $a(\mathbf{z}, \overline{\mathbf{z}})$ is the variational form for the structural part and $\ell(\overline{\mathbf{z}})$ is a work done by an external force through variational displacement, and Z is the space of kinematically admissible virtual displacement. The variational form and linearized form for structure are provided in the reference (Kim et al., 2000). Let the current configuration be t_n and k is the last iteration counter. Assuming that the external force is independent of the displacement, the linearized incremental equation of Eq. (21) is obtained as

$$a^*(^n\mathbf{z}^k;\ \Delta\mathbf{z}^{k+1},\ \overline{\mathbf{z}}) + b^*(^n\mathbf{z}^k;\ \Delta\mathbf{z}^{k+1},\ \overline{\mathbf{z}})$$
$$= \ell(\overline{\mathbf{z}}) - a(^n\mathbf{z}^k,\ \overline{\mathbf{z}}) - b(^n\mathbf{z}^k,\ \overline{\mathbf{z}}), \quad \forall \overline{\mathbf{z}} \in Z \tag{22}$$

which is linear in incremental displacement for a given displacement variation. The linearized system Eq. (22) is solved iteratively for the incremental displacement until the residual forces (right side of Eq. (22)) become zero at each load step. The path dependency of the problem comes from the tangential slip function.

Design Sensitivity Analysis of Frictional Contact Problem

Consider the governing variational equation at t_n for the perturbed shape design Ω_τ as

$$a_{\Omega_\tau}(\mathbf{z}_\tau,\overline{\mathbf{z}}_\tau) + b_{\Gamma_{c_\tau}}(\mathbf{z}_\tau,\overline{\mathbf{z}}_\tau) = \ell_{\Omega_\tau}(\overline{\mathbf{z}}_\tau), \quad \forall \overline{\mathbf{z}}_\tau \in Z_\tau \tag{23}$$

The derivative of the normal contact variational form in Eq. (23) at the perturbed boundary Γ_τ can be obtained as

$$\tfrac{d}{d\tau}[b_N(\mathbf{z},\overline{\mathbf{z}})] = b_N^*(\mathbf{z};\dot{\mathbf{z}},\overline{\mathbf{z}}) + b_N'(\mathbf{z},\overline{\mathbf{z}}) \tag{24a}$$

where $b_N^*(\mathbf{z};\dot{\mathbf{z}},\overline{\mathbf{z}})$ is the linearized normal contact bilinear form (Kim et al., 2000),

$$b_N^*(\mathbf{z};\dot{\mathbf{z}},\overline{\mathbf{z}}) \equiv \omega_n \int_{\Gamma_c} (\hat{\overline{\mathbf{z}}}^T \mathbf{e}_n \mathbf{e}_n{}^T \dot{\hat{\mathbf{z}}} - (\alpha g_n / c) \hat{\overline{\mathbf{z}}}^T \mathbf{e}_t \mathbf{e}_t{}^T \dot{\hat{\mathbf{z}}}) \, d\Gamma$$
$$- \omega_n \int_{\Gamma_c} (g_n \|\mathbf{t}\| / c)(\hat{\overline{\mathbf{z}}}^T \mathbf{e}_t \mathbf{e}_n{}^T \dot{\mathbf{z}}_{c,\xi} + \overline{\mathbf{z}}_{c,\xi}{}^T \mathbf{e}_n \mathbf{e}_t{}^T \dot{\hat{\mathbf{z}}}) \, d\Gamma \tag{24b}$$
$$- \omega_n \int_{\Gamma_c} (g_n{}^2 / c) \overline{\mathbf{z}}_{c,\xi}{}^T \mathbf{e}_n \mathbf{e}_n{}^T \dot{\mathbf{z}}_{c,\xi} \, d\Gamma$$

and $b_N'(\mathbf{z},\overline{\mathbf{z}})$ is the normal contact fictitious load form

$$b_N'(\mathbf{z},\overline{\mathbf{z}}) = b_N^*(\mathbf{z};\mathbf{V},\overline{\mathbf{z}}) + \omega_n \int_{\Gamma_c} \kappa g_n \hat{\overline{\mathbf{z}}}^T \mathbf{e}_n (\mathbf{V}^T \mathbf{n}) \, d\Gamma \tag{24c}$$

which depends explicitly on the design velocity field. The material derivative of the tangential stick variational form in Eq. (18c) at the perturbed configuration becomes

$$\tfrac{d}{d\tau}[b_T(\mathbf{z},\overline{\mathbf{z}})] = b_T^*(\mathbf{z};\dot{\mathbf{z}},\overline{\mathbf{z}}) + b_T'(\mathbf{z},\overline{\mathbf{z}}) \tag{25a}$$

where $b_T^*(\mathbf{z};\dot{\mathbf{z}},\overline{\mathbf{z}})$ is the linearized tangential stick bilinear form (Kim et al., 2000),

$b_T^*(\mathbf{z};\dot{\mathbf{z}},\overline{\mathbf{z}})$

$= \omega_t \int_{\Gamma_c} \left(v^2 + (vg_t/c^2)((\gamma\|\mathbf{t}\| - 2\alpha\beta)g_n - \beta\|\mathbf{t}\|^2) \right)(\hat{\overline{\mathbf{z}}}^T\mathbf{e}_t\mathbf{e}_t^T\dot{\hat{\mathbf{z}}})d\Gamma$

$+\omega_t \int_{\Gamma_c} \|\mathbf{t}^0\|g_n \left(v/c - g_t(2\beta\|\mathbf{t}\|^2 + \alpha\beta g_n - \gamma g_n\|\mathbf{t}\|)/c^3 \right)\hat{\overline{\mathbf{z}}}^T\mathbf{e}_n\mathbf{e}_n^T\dot{\mathbf{z}}_{c,\xi}\,d\Gamma$

$+\omega_t \int_{\Gamma_c} \|\mathbf{t}^0\|g_n \left(v/c - g_t(2\beta\|\mathbf{t}\|^2 + \alpha\beta g_n - \gamma g_n\|\mathbf{t}\|)/c^3 \right)\overline{\mathbf{z}}_{c,\xi}^T\mathbf{e}_n\mathbf{e}_n^T\dot{\hat{\mathbf{z}}}\,d\Gamma$

$+\omega_t \int_{\Gamma_c} (\alpha vg_t/c)\hat{\overline{\mathbf{z}}}^T(\mathbf{e}_n\mathbf{e}_t^T + \mathbf{e}_t\mathbf{e}_n^T)\dot{\hat{\mathbf{z}}}\,d\Gamma$

$+\omega_t \int_{\Gamma_c} (vg_t\|\mathbf{t}\|/c)(\hat{\overline{\mathbf{z}}}^T\mathbf{e}_n\mathbf{e}_n^T\dot{\mathbf{z}}_{c,\xi} + \overline{\mathbf{z}}_{c,\xi}^T\mathbf{e}_n\mathbf{e}_n^T\dot{\hat{\mathbf{z}}})d\Gamma$

$+\omega_t \int_{\Gamma_c} \left(g_t(\|\mathbf{t}^0\| - 2v\|\mathbf{t}\|)/c \right)(\hat{\overline{\mathbf{z}}}^T\mathbf{e}_n\mathbf{e}_n^T\dot{\mathbf{z}}_{c,\xi} + \overline{\mathbf{z}}_{c,\xi}^T\mathbf{e}_n\mathbf{e}_n^T\dot{\hat{\mathbf{z}}})d\Gamma$

$+\omega_t \int_{\Gamma_c} \left((g_n\|\mathbf{t}^0\|/c)^2 - (g_ng_t\|\mathbf{t}^0\|/c^3)(3\beta g_n\|\mathbf{t}\| - \gamma g_n^2) \right)\overline{\mathbf{z}}_{c,\xi}^T\mathbf{e}_n\mathbf{e}_n^T\dot{\mathbf{z}}_{c,\xi}\,d\Gamma$

$-\omega_t \int_{\Gamma_c} (2g_ng_tv/c)\overline{\mathbf{z}}_{c,\xi}^T(\mathbf{e}_n\mathbf{e}_t^T + \mathbf{e}_t\mathbf{e}_n^T)\dot{\mathbf{z}}_{c,\xi}\,d\Gamma$

$+\omega_t \int_{\Gamma_c} (g_ng_tv/c)(\hat{\overline{\mathbf{z}}}^T\mathbf{e}_t\mathbf{e}_n^T\dot{\mathbf{z}}_{c,\xi\xi} + \overline{\mathbf{z}}_{c,\xi\xi}^T\mathbf{e}_n\mathbf{e}_t^T\dot{\hat{\mathbf{z}}})d\Gamma$

$+\omega_t \int_{\Gamma_c} (g_n^2g_t\|\mathbf{t}^0\|/c^2)(\overline{\mathbf{z}}_{c,\xi}^T\mathbf{e}_n\mathbf{e}_n^T\dot{\mathbf{z}}_{c,\xi\xi} + \overline{\mathbf{z}}_{c,\xi\xi}^T\mathbf{e}_n\mathbf{e}_n^T\dot{\mathbf{z}}_{c,\xi})d\Gamma$

(25b)

and $b_T'(\mathbf{z},\overline{\mathbf{z}})$ is the tangential stick fictitious load form defined as

$b_T'(\mathbf{z},\overline{\mathbf{z}}) = b_T^*(\mathbf{z};\mathbf{V},\overline{\mathbf{z}})$

$+\omega_t \int_{\Gamma_c} (2g_t\|\mathbf{t}\|/c)\hat{\overline{\mathbf{z}}}^T\mathbf{e}_t\mathbf{e}_t^{0T}(\mathbf{V}_{c,\xi} + \dot{\mathbf{z}}_{c,\xi}^0)d\Gamma$

$+\omega_t \int_{\Gamma_c} (v(2\beta^0g_t - \|\mathbf{t}^0\|^2))\hat{\overline{\mathbf{z}}}^T\mathbf{e}_t\mathbf{e}_t^{0T}(\hat{\mathbf{V}} + \hat{\mathbf{z}}^0)d\Gamma$

$+\omega_t \int_{\Gamma_c} \left(\beta^0g_ng_t(\|\mathbf{t}^0\| + \|\mathbf{t}\|)/cc^0 \right)\hat{\overline{\mathbf{z}}}^T\mathbf{e}_t\mathbf{e}_n^{0T}(\mathbf{V}_{c,\xi} + \dot{\mathbf{z}}_{c,\xi}^0)d\Gamma$

$-\omega_t \int_{\Gamma_c} (g_n\|\mathbf{t}\|\|\mathbf{t}^0\|^2/cc^0)\hat{\overline{\mathbf{z}}}^T\mathbf{e}_t\mathbf{e}_n^{0T}(\mathbf{V}_{c,\xi} + \dot{\mathbf{z}}_{c,\xi}^0)d\Gamma$

$+\omega_t \int_{\Gamma_c} \left(g_n\|\mathbf{t}^0\|(2\beta^0g_t - \|\mathbf{t}^0\|^2)/cc^0 \right)\overline{\mathbf{z}}_{c,\xi}^T\mathbf{e}_n\mathbf{e}_t^{0T}(\hat{\mathbf{V}} + \hat{\mathbf{z}}^0)d\Gamma$

$+\omega_t \int_{\Gamma_c} \left(g_ng_n^0(2\beta^0g_t - \|\mathbf{t}^0\|^2)/cc^0 \right)\overline{\mathbf{z}}_{c,\xi}^T\mathbf{e}_n\mathbf{e}_n^{0T}(\mathbf{V}_{c,\xi} + \dot{\mathbf{z}}_{c,\xi}^0)d\Gamma$

$+\omega_t \int_{\Gamma_c} \kappa\left(vg_t\hat{\overline{\mathbf{z}}}^T\mathbf{e}_t + (g_ng_t\|\mathbf{t}^0\|/c)\hat{\overline{\mathbf{z}}}^T\mathbf{e}_t \right)(\mathbf{V}^T\mathbf{n})d\Gamma$

(25c)

The material derivative of the tangential slip variational form of Eq. (20) can be taken using the similar procedure as in the stick condition, except the normal gap function, to obtain Eq. (25a) where $b_T^*(\mathbf{z};\dot{\mathbf{z}},\overline{\mathbf{z}})$ is obtained from the linearized tangential slip bilinear form (Kim et al., 2000)

$b_T^*(\mathbf{z};\dot{\mathbf{z}},\overline{\mathbf{z}})$

$\equiv \omega_t \int_{\Gamma_c} v\hat{\overline{\mathbf{z}}}^T\mathbf{e}_t\mathbf{e}_n^T\dot{\hat{\mathbf{z}}}d\Gamma$

$+\omega_t \int_{\Gamma_c} (vg_n/c^2)\left((\gamma\|\mathbf{t}\| - 2\alpha\beta)g_n - \beta\|\mathbf{t}\|^2 \right)\hat{\overline{\mathbf{z}}}^T\mathbf{e}_t\mathbf{e}_t^T\dot{\hat{\mathbf{z}}}d\Gamma$

$-\omega_t \int_{\Gamma_c} \|\mathbf{t}^0\|\left(g_n^2(2\beta\|\mathbf{t}\|^2 + \alpha\beta g_n - \gamma g_n\|\mathbf{t}\|)/c^3 \right)(\hat{\overline{\mathbf{z}}}^T\mathbf{e}_t\mathbf{e}_n^T\dot{\mathbf{z}}_{c,\xi} + \overline{\mathbf{z}}_{c,\xi}^T\mathbf{e}_n\mathbf{e}_t^T\dot{\hat{\mathbf{z}}})d\Gamma$

$+\omega_t \int_{\Gamma_c} (\alpha vg_n/c)\hat{\overline{\mathbf{z}}}^T(\mathbf{e}_n\mathbf{e}_t^T + \mathbf{e}_t\mathbf{e}_n^T)\dot{\hat{\mathbf{z}}}d\Gamma$

$+\omega_t \int_{\Gamma_c} (vg_n\|\mathbf{t}\|/c)\hat{\overline{\mathbf{z}}}^T\mathbf{e}_n\mathbf{e}_n^T\dot{\mathbf{z}}_{c,\xi}\,d\Gamma$

$+\omega_t \int_{\Gamma_c} (g_n(v\|\mathbf{t}\| + \|\mathbf{t}^0\|)/c)\overline{\mathbf{z}}_{c,\xi}^T\mathbf{e}_n\mathbf{e}_n^T\dot{\hat{\mathbf{z}}}d\Gamma$

$+\omega_t \int_{\Gamma_c} \left(g_n(\|\mathbf{t}^0\| - 2v\|\mathbf{t}\|)/c \right)(\hat{\overline{\mathbf{z}}}^T\mathbf{e}_n\mathbf{e}_n^T\dot{\mathbf{z}}_{c,\xi} + \overline{\mathbf{z}}_{c,\xi}^T\mathbf{e}_n\mathbf{e}_n^T\dot{\hat{\mathbf{z}}})d\Gamma$

$-\omega_t \int_{\Gamma_c} \left((g_n^2\|\mathbf{t}^0\|/c^3)(3\beta g_n\|\mathbf{t}\| - \gamma g_n^2) \right)\overline{\mathbf{z}}_{c,\xi}^T\mathbf{e}_n\mathbf{e}_n^T\dot{\mathbf{z}}_{c,\xi}\,d\Gamma$

$-\omega_t \int_{\Gamma_c} (2g_n^2v/c)\overline{\mathbf{z}}_{c,\xi}^T(\mathbf{e}_n\mathbf{e}_t^T + \mathbf{e}_t\mathbf{e}_n^T)\dot{\mathbf{z}}_{c,\xi}\,d\Gamma$

$+\omega_t \int_{\Gamma_c} (g_n^2v/c)(\hat{\overline{\mathbf{z}}}^T\mathbf{e}_t\mathbf{e}_n^T\dot{\mathbf{z}}_{c,\xi\xi} + \overline{\mathbf{z}}_{c,\xi\xi}^T\mathbf{e}_n\mathbf{e}_t^T\dot{\hat{\mathbf{z}}})d\Gamma$

$+\omega_t \int_{\Gamma_c} (g_n^3\|\mathbf{t}^0\|/c^2)(\overline{\mathbf{z}}_{c,\xi}^T\mathbf{e}_n\mathbf{e}_n^T\dot{\mathbf{z}}_{c,\xi\xi} + \overline{\mathbf{z}}_{c,\xi\xi}^T\mathbf{e}_n\mathbf{e}_n^T\dot{\mathbf{z}}_{c,\xi})d\Gamma$

(26a)

and $b_T'(\mathbf{z},\overline{\mathbf{z}})$ is the tangential slip fictitious load form defined as

$b_T'(\mathbf{z},\overline{\mathbf{z}}) \equiv b_T^*(\mathbf{z};\mathbf{V},\overline{\mathbf{z}})$

$+\omega_t \int_{\Gamma_c} (g_n\|\mathbf{t}\|/c)\hat{\overline{\mathbf{z}}}^T\mathbf{e}_t\mathbf{e}_t^{0T}(\mathbf{V}_{c,\xi} + \dot{\mathbf{z}}_{c,\xi}^0)d\Gamma$

$+\omega_t \int_{\Gamma_c} (v\beta^0g_n/c^0)\hat{\overline{\mathbf{z}}}^T\mathbf{e}_t\mathbf{e}_t^{0T}(\hat{\mathbf{V}} + \hat{\mathbf{z}}^0)d\Gamma$

$+\omega_t \int_{\Gamma_c} (\beta^0g_ng_0\|\mathbf{t}^0\|/cc^0)\hat{\overline{\mathbf{z}}}^T\mathbf{e}_t\mathbf{e}_n^{0T}(\mathbf{V}_{c,\xi} + \dot{\mathbf{z}}_{c,\xi}^0)d\Gamma$

$+\omega_t \int_{\Gamma_c} (g_n^2/c)\overline{\mathbf{z}}_{c,\xi}^T\mathbf{e}_n\mathbf{e}_t^{0T}(\mathbf{V}_{c,\xi} + \dot{\mathbf{z}}_{c,\xi}^0)d\Gamma$

$+\omega_t \int_{\Gamma_c} (\beta^0\|\mathbf{t}^0\|g_n^2/cc^0)\overline{\mathbf{z}}_{c,\xi}^T\mathbf{e}_n\mathbf{e}_t^{0T}(\hat{\mathbf{V}} + \hat{\mathbf{z}}^0)d\Gamma$

$+\omega_t \int_{\Gamma_c} (\beta^0g_n^2g_n^0/cc^0)\overline{\mathbf{z}}_{c,\xi}^T\mathbf{e}_n\mathbf{e}_n^{0T}(\mathbf{V}_{c,\xi} + \dot{\mathbf{z}}_{c,\xi}^0)d\Gamma$

$+\omega_t \int_{\Gamma_c} \kappa(vg_n\hat{\overline{\mathbf{z}}}^T\mathbf{e}_t + (g_n^2\|\mathbf{t}^0\|/c)\overline{\mathbf{z}}_{c,\xi}^T\mathbf{e}_n)(\mathbf{V}^T\mathbf{n})d\Gamma$

(26b)

Note that the same symbol $b_T'(\mathbf{z},\overline{\mathbf{z}})$ is used for stick and slip conditions. Thus, the material derivative of the contact variational form can be obtained by combining Eqs. (24a), (25a), (25b) and (25c) for the stick condition and Eqs. (24a), (26a), and (26b) for the slip condition,

$$\frac{d}{d\tau}[b_{\Gamma_c}(\mathbf{z},\overline{\mathbf{z}})] = b_{\Gamma_c}^*(\mathbf{z};\dot{\mathbf{z}},\overline{\mathbf{z}}) + b_V'(\mathbf{z},\overline{\mathbf{z}}) \qquad (27a)$$

where

$$b_{\Gamma_c}^*(\mathbf{z};\dot{\mathbf{z}},\overline{\mathbf{z}}) = b_N^*(\mathbf{z};\dot{\mathbf{z}},\overline{\mathbf{z}}) + b_T^*(\mathbf{z};\dot{\mathbf{z}},\overline{\mathbf{z}}) \qquad (27b)$$
$$b_V'(\mathbf{z},\overline{\mathbf{z}}) = b_N'(\mathbf{z},\overline{\mathbf{z}}) + b_T'(\mathbf{z},\overline{\mathbf{z}}) \qquad (27c)$$

By collecting all the terms, the following linear system of equations can be obtained

$$a_\Omega^*(^n\mathbf{z};{}^n\dot{\mathbf{z}},\overline{\mathbf{z}}) + b_{\Gamma_c}^*(^n\mathbf{z};{}^n\dot{\mathbf{z}},\overline{\mathbf{z}}) = \ell_V'(\overline{\mathbf{z}}) - a_V'(^n\mathbf{z},\overline{\mathbf{z}}) - b_V'(^n\mathbf{z},\overline{\mathbf{z}})$$
$$\forall \overline{\mathbf{z}} \in Z \qquad (28)$$

The left side of Eq. (28) is the same form as in Eq. (22). Thus, the same decomposed stiffness matrix can be used for computation of the material derivative of the displacement with the fictitious load. Since the tangent stiffness operator in Eq. (22) is not symmetric, the direct differentiation method is more suitable. Since the tangential slip fictitious load depends on the material derivative of the previous converged configuration, the linear system Eq. (28) is solved at each load step. Sensitivity computation does not require convergence iterations; only the stiffness matrix at the converged configuration of each load step is used for linear analysis.

RBDO PROCESS

Solving an RBDO problem is computationally expensive since it requires reliability analysis for each constraint functions, and within each RBDO design iteration, many constraint functions may have to be evaluated. In this paper, an approximated method and active constraint set strategy are used to develop an efficient RBDO by reducing the number of reliability index evaluation.

Two-Point Approximation Method

To improve efficiency of RBDO process, the two-point approximation (TPA) method (Wang and Grandhi, 1994) is employed using the nonlinearity index. To use TPA, the intermediate random variables y_i are introduced as

$$y_i = x_i^{p_i}, \quad i=1,2, ..., n \qquad (29)$$

where p_i is the nonlinearity index for the ith random variable which is different from the uniform index used by Wang and Grandi (1994).

Let $^m\mathbf{x}$ and $^m\mathbf{y}$ be the current MPP point and the corresponding intermediate random vector, respectively. Taking the first-order Taylor approximation of the G function at $^m\mathbf{y}$,

$$G(\mathbf{y}) = G(^m\mathbf{y}) + \sum_{i=1}^{n}(y_i - {}^m y_i)\frac{\partial G(^m\mathbf{y})}{\partial y_i} \qquad (30)$$

where $\mathbf{y}$ is the intermediate random vector of the random vector $\mathbf{x}$. Substituting Eq. (29) to Eq. (30),

$$G(\mathbf{x}) = G(^m\mathbf{x}) + \sum_{i=1}^{n}\left((x_i)^{p_i} - ({}^m x_i)^{p_i}\right)\frac{\partial G(^m\mathbf{x})/\partial x_i}{\partial y_i/\partial x_i} \qquad (31)$$

where $\partial y_i/\partial x_i$ at $^m\mathbf{x}$ can be evaluated as,

$$\left.\frac{\partial y_i}{\partial x_i}\right|_{x={}^m x} = \left.\frac{\partial x_i^{p_i}}{\partial x_i}\right|_{x={}^m x} = p_i(^m x_i)^{(p_i-1)} \qquad (32)$$

substituting Eq. (32) into Eq. (31),

$$G_{TPA}(\mathbf{x}) = G(^m\mathbf{x}) + \sum_{i=1}^{n}\left((x_i)^{p_i} - ({}^m x_i)^{p_i}\right)\frac{\partial G(^m\mathbf{x})/\partial x_i}{p_i(^m x_i)^{(p_i-1)}}$$
$$(33a)$$

Thus, using Eq. (33a), the derivatives at any point $\mathbf{x}$ can be expressed as

$$\frac{\partial G_{TPA}(\mathbf{x})}{\partial x_i} = \left(\frac{x_i}{^m x_i}\right)^{p_i-1}\frac{\partial G(^m\mathbf{x})}{\partial x_i} \qquad (33b)$$

Since the derivatives at the previous MPP $^{m-1}\mathbf{x}$ have been calculated during the MPP search process, Eq. (33a) should be equal to this value, i.e.,

$$\left(\frac{^{m-1}x_i}{^m x_i}\right)^{p_i-1}\frac{\partial G(^m\mathbf{x})}{\partial x_i} = \frac{\partial G(^{m-1}\mathbf{x})}{\partial x_i} \qquad (34)$$

From Eq. (34), value of p_i can be calculated for each random variable x_i, i.e.,

$$p_i = 1 + \frac{\log\left(\dfrac{\partial G(^{m-1}\mathbf{x})/\partial x_i}{\partial G(^m\mathbf{x})/\partial x_i}\right)}{\log(^{m-1}x_i/^m x_i)} \qquad (35)$$

then, the TPA function is Eq. (31).

RBDO Algorithm

The main steps of the proposed RBDO algorithm, as shown in Fig. 3, are summarized as:

(1) Perform reliability analysis at the current design $\mathbf{d}^k$ using the mean value first-order second moment reliability method (MVFO) for all constraints functions.

(2) Identify the set of critical constraints using normalized form,

$$\overline{\xi}_i = \frac{\beta_{si}(\mathbf{d}^k) - \beta_i^{min}}{\beta_i^{min}} > \xi; \quad \text{Inactive} \qquad (36a)$$

$$\overline{\xi}_i = \frac{\beta_{si}(\mathbf{d}^k) - \beta_i^{min}}{\beta_i^{min}} \leq \xi; \quad \text{Critical} \qquad (36b)$$

Since β_{si} is obtained from MVFO and may not be accurate, to make the proposed RBDO algorithm robust, it is desirable to choose a relatively larger positive value ξ compared with deterministic structural optimization, e.g., $0.25 \leq \xi \leq 1.5$

(3) For the critical constraints identified in Step 2, compute accurate critical reliability indices using FORM.

(4) The reliability-based DSA can be obtained as

$$\frac{\partial \beta_s(\mathbf{d}^k)}{\partial d_i} = \frac{1}{\beta_s}\mathbf{u}_{g=0}^{*T}\frac{\partial T(\mathbf{x}_{g=0}^*,\mathbf{d}^k)}{\partial d_i} \qquad (37)$$

where $\mathbf{u}_{g=0}^*$ is the MPP in $\mathbf{u}$-space and T is the transformation in FORM between the $\mathbf{x}$-space and the $\mathbf{u}$-space at design $\mathbf{d}^k$

(5) In the second-level approximation process, the nonlinearity index of the jth critical reliability constraints with respect to the ith design variable can be obtained as

$$p_i^j = 1 + \frac{\log\left(\dfrac{\partial \beta_{sj}(^{m-1}\mathbf{d}^k)/\partial d_i}{\partial \beta_{sj}(^m\mathbf{d}^k)/\partial d_i}\right)}{\log(^{m-1}d_i/^m d_i)}, \quad j \in J \qquad (38)$$

where J is the set of critical constraints. The jth approximate reliability index can be obtained using TPA,

$$[\beta_{sj}]_{TPA}(\mathbf{d}^k) = \beta_{sj}(^m\mathbf{d}^k)$$

$$+ \sum_{i=1}^{n1} \left[(d_i^k)^{p_i^j} - (^m d_i^k)^{p_i^j} \right] \frac{\partial \beta_{sj}(^m \mathbf{d}^k) / \partial d_i}{p_i^j (^m d_i^k)^{(p_i^j - 1)}} \quad (39)$$

An approximate problem of the RBDO problem corresponding to Eqs. (4a) to (4c) is obtained as

$$\min \ W(\mathbf{d}^k)$$
$$\text{s.t. } [\beta_{sj}]_{TPA}(\mathbf{d}^k) \geq \beta_j^{\min}, \ j \in J \quad (40)$$
$$\Delta d_i^k \leq d_i^k - {}^m d_i^k \leq \Delta d_i^k, \ i = 1,2,..., \ n1$$

where Δd_i^k is positive move limits used to improve robustness of RBDO.

Numerical Example

Figure 4 shows the initial geometry of a rubber plate punch problem with a cylindrical rigid punch. The radius of the rigid punch is 8.0 cm. The lower right rigid wall is fixed and the upper left punch moves downward 9.0 cm. The domain is discretized using 93 RKPM particles and 40 piecewise linear master segments. The Mooney-Rivlin type hyper-elastic material is used with a pressure projection formulation for nearly incompressibility constraints. Material constants $C_{10} = 80$ kPa, $C_{01} = 20$ kPa and bulk modulus $K = 80$ MPa are used. Frictional contact constraints are imposed between the rubber plate and rigid wall with a friction coefficient of $\mu = 0.2$.

The random variables and their statistical distributions are listed in Table 1. The design sensitivity analysis starts from choosing design parameters and computing design velocity fields for shape design parameters. First design parameter d_1 is the mean value of the upper boundary movement (x_1) of the plate, and second design parameter d_2 is the mean value of the radius (x_2) of the right lower rigid wall.

Then design sensitivities of reliability indices with respect to design variable d_i are shown in the fifth column in Table 2. The finite differece results are shown in the fourth column for 1% perturbation of each design variable d_i. The sixth column is the agreement between $\Delta \Psi$ and Ψ'. The results obtained by the proposed method agree very well with those obtained by the finite difference method.

The objective of the design problem is to reduce the maximum von Mises stress at Element 2 of the plate by changing design variables. The stress failure functions are defined at Elements 4, 57, and 59 as $g_i(\mathbf{X}) = \sigma_i(\mathbf{X}) - \sigma_{ti}$ where $\sigma_{t1} = 85.1$, $\sigma_{t2} = 85.2$, and $\sigma_{t3} = 80.3$. The probabilistic constraints are the failure probability of the von Mises stresses at Elements 4, 57, and 59 with upper bound $\beta_{t1} = \beta_{t2} = \beta_{t3} = 3.096$ (i.e., $P_f = 0.1\%$, or the required reliability is 99.9%) as shown in Table 3. The design optimization problem is

$$\min \ \sigma_2$$
$$\text{s.t. } [\beta_{s1}]_{TPA} \geq \beta_{t1}$$
$$[\beta_{s2}]_{TPA} \geq \beta_{t2}$$
$$[\beta_{s3}]_{TPA} \geq \beta_{t3}$$
$$\Delta d_i^k \leq d_i^k - {}^m d_i^k \leq \Delta d_i^k, \ i = 1,2,3$$

Table 3 shows that the initial design is an infeasiable design since the first and second constraints are violated. A feasible design is obtained using the proposed RBDO method as shown in the fourth column in Table 3. The modified feasible direction method (MFD) is employed in the second-level approximation process during RBDO. The deformed shape of the optimal design at the final time step with von Mises stress countour is shown in Fig. 5.

CONCLUSION

An efficient method was developed for reliability-based shape design optimization for a hyper-elastic structure with frictional contact using the meshfree method. The first-order reliability method was utilized for reliability analysis. For overall RBDO, reliability indices are used to represent the probabilistic constraints. To develop the continuum-based DSA for the hyper-elastic constitutive relation and penalized contact formulation, the material derivative of continuum mechanics is utilized. A numerical result is presented to validate the proposed method.

REFERENCES

Arora, J.S., 1989, *Introduction to Optimum Design*, McGraw-Hill, New York, NY.

Breitung, K., 1984, "Asymptotic Approximations for Multinormal Integrals," *Journal of Engineering Mechanics*, Vol. 110(3), pp. 357-366.

Chandu, S.V.L. and Grandhi, R.V., 1995, "General Purpose Procedure for Reliability Based Structural Optimization under Parametric Uncertainties," *Advances in Engineering Software*, Vol. 23, pp. 7-14.

Chang, T.Y.P., Saleeb, A.F., and Li, G., 1991, "Large Strain Analysis of Rubber-like Materials Based on a Perturbed Lagrangian Variational Principles," *Computational Mechanics*, Vol. 8, pp. 221-233.

Chen, J. S., Wu, C. T., and Pan, C., 1996, "A Pressure Projection Method for Nearly Incompressible Rubber Hyper-elasticity, Part I: Theory and Part II: Application," *ASME Journal of Applied Mechanics (63)*, pp. 862-876.

Chen, J. S., Wu, C. T., and Pan, C., "Application of Reproducing Kernel Particle Method to Large Deformation and Contact Analysis of Elastomers," *Rubber Chemistry and Technology*, Vol. 71, pp. 191-213, 1998.

Enevoldsen, I., 1994, "Reliability-Based Optimization as an Information Tool," *Mech. Struct. & Mach.*, Vol. 22(1), pp. 117-135.

Enevoldsen, I. and Sorensen, J.D., 1994, "Reliability-Based Optimization in Structural Engineering," *Structural Safety*, Vol. 15, pp. 169-196.

Frangopol, D.M. and Corotis, R.B., 1996, "Reliability-Based Structural System Optimization: State-of-the-Art versus State-of-the-Practice," *Analysis and Computation: Proceedings of the Twelfth Conference held in Conjunction with Structures Congress XIV*, F.Y. Cheng, ed., pp. 67-78.

Grandhi, R.V. and Wang, L.P., 1998, "Reliability-Based Structural Optimization Using Improved Two-Point Adaptive Nonlinear Approximations*," Finite Elements in Analysis and Design*, Vol. 29, pp. 35-48.

Haftka, R.T. and Gurdal, Z., 1991, *Elements of Structural Optimization*, Klumer Academic Publications, Dordrecht, Netherlands.

Hughes, T.J.R., 1987, *The Finite Element Method*, Prentice-Hall, Englewood, Cliffs, NJ.

Hohenbichler, M. and Rackwitz, R., 1981, "Nonnormal Dependent Vectors in Structural Reliability," *Journal of the Engineering Mechanics Division*, ASCE, 107(6), 1227-1238.

Kim, Nam Ho, Park, Young Ho, Choi, Kyung Kook, 2000 (to appear), "Optimization of Hyper-Elastic Structure with Multibody Contact Using Continuum-Based Shape Design Sensitivity Analysis," *Structural Optimization*.

Liu, W. K., Jun, S., and Zhang, Y. F., 1995, "Reproducing Kernel Particle Methods," *Int. J. Num. Methods in Fluids* (20), pp. 1081-1106.

Madsen, H.O., Krenk, S., and Lind, N.C., 1986, *Methods of Structural Safety*, Prentice-Hall, Englewood Cliffs, NJ.

Rubinstein, R.Y., 1981, *Simulation and the Monte Carlo Method*, John Wiley and Sons, New York, NY.

Tu, Jian, Choi, Kyung K., and Park, Young H., 1999, "A New Study on Reliability Based Design Optimization," *CASME Journal of Mechanical Design*, Vol. 121(4).

Tvedt, L., 1990, "Distribution of Quadratic Forms in Normal Space-Application to Structural Reliability," *Journal of Engineering Mechanics*, Vol. 116(6), pp. 1183-1197.

Wang, L. and Grandhi, R., 1994, "Efficient Safety Index Calculation For Structural Reliability Analysis," *Computers and Structures*, Vol. 52(1).

Wriggers, P., Van, T.V., and Stein, E., 1990, "Finite Element Formulation of Large Deformation Impact-Contact Problems with Friction," *Computers and Structures*, Vol. 37, pp. 319-331.

Wu, Y.T. and Wirsching, P.H., 1987, "New Algorithm for Structural Reliability Estimation," *Journal of Engineering Mechanics*, Vol. 113(9), pp. 1319-1336.

Wu, Y.T., Millwater, H.R., and Cruse, T.A., 1990, "An Advanced Probabilistic Structural Analysis Method for Implicit Performance Functions," *AIAA Journal*, Vol. 28(9), pp. 1663-1669.

Wu, Y.T. and Wang, W., 1996, "A New Method for Efficient Reliability-Based Design Optimization," *Probabilistic Mechanics & Structural Reliability: Proceedings of the 7th Special Conference*, pp. 274-277.

Yu, X., Choi, K.K., and Chang, K.H., 1997, "A Mixed Design Approach for Probabilistic Structural Durability," *Journal of Structural Optimization*, Vol. 14, No. 2-3, pp. 81-90.

Table 1. Sensitivity Analysis Results and Comparison with Finite Difference Method

Randon Variables	Mean Value	Standard Deviation	Distribution
x_1	0.0	0.01	Normal
x_2	8.0	0.01	Normal

Table 2. Random Variable Description

Performance	DV	Ψ	$\Delta\Psi$	Ψ'	$(\Delta\Psi / \Psi') \times 100\%$
β_{s1}	d_1	2.3339	-9.966×10^2	-9.966×10^2	100.0%
β_{s2}	d_1	2.3054	-9.974×10^2	-9.974×10^2	100.0%
β_{s1}	d_2	2.3339	8.227×10^1	8.235×10^1	99.9%
β_{s2}	d_2	2.3054	7.238×10^1	7.228×10^1	99.9%

Table 3. Cost and Constraint Function Values at Initial and Optimum Design

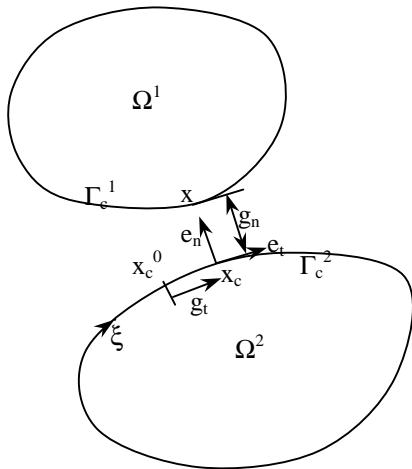| Fucntion	Decsription	initial $P_f=\Phi(-\beta)$	optimum $P_f=\Phi(-\beta)$	change
Cost	stress at element 2	119.179	120.502	1.1 %
Constraint (g_1)	stress at element 59	0.98 %	0.09 %	−90.8 %
Constraint (g_2)	stress at element 57	1.06 %	0.10 %	−90.6 %
Constraint (g_3)	stress at element 4	5.569×10^{-13} %	1.246×10^{-11} %	2137.4 %

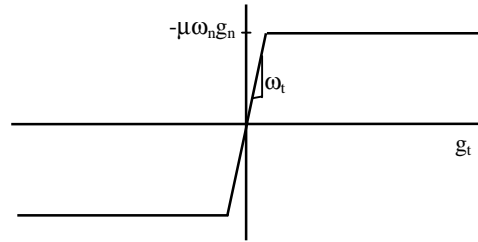**Figure 1. Multibody Contact Condition**

Figure 2. Frictional Interface Model
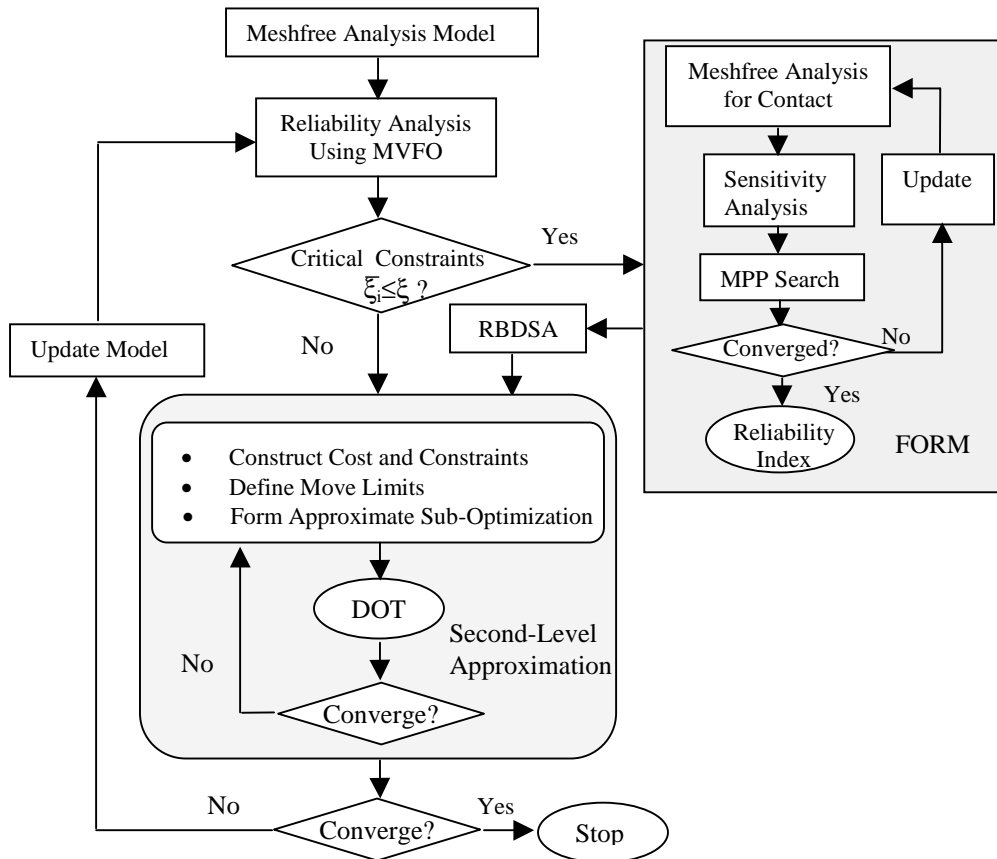

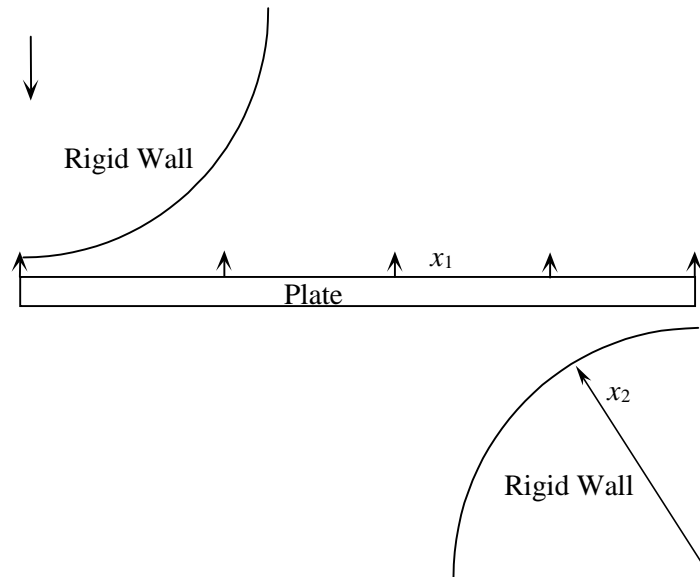**Figure 3. RBDO Algorithm**

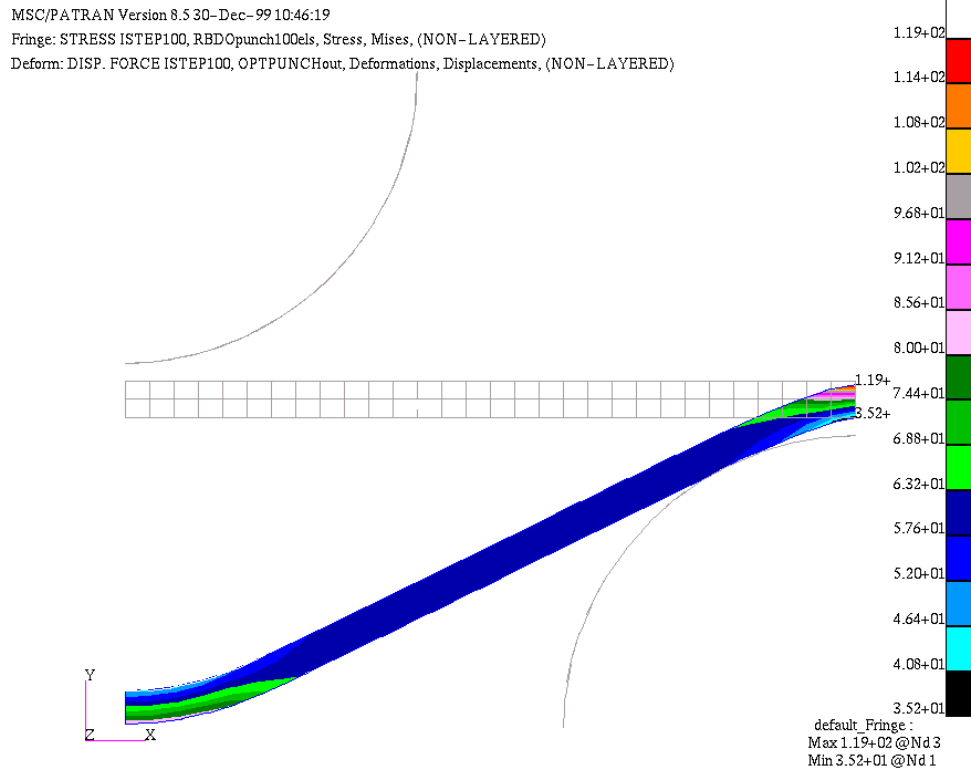**Figure 4. Geometry and Design Parameterization of Plate Punch Problem**

Figure 5. Deformed von Mises Stress Contour Plot for Optimal Design